

Experimental investigation of resonant excitation of slow low-frequency waves in a plasma by opposed electron beams

V. D. Fedorchenko, Yu. P. Mazalov, and A. S. Bakal

Physicotechnical Institute, Academy of Sciences of the Ukrainian SSR, Kharkov
(Submitted 18 August 1979)
Zh. Eksp. Teor. Fiz. 78, 2238–2250 (June 1980)

An investigation was made of the excitation of space-charge waves in a double-beam plasma system, of the mechanism of plasma expansion by the ponderomotive force of high-frequency oscillations, and of the process of excitation of ion-acoustic oscillations as a result of mixing of space-charge waves. Strong expulsion of the plasma in the region of the maximum density of hf oscillations ($\delta n/n \sim 0.9$) was observed in the case of resonant mode merging. The process excited intense ion-acoustic waves whose amplitudes were sufficient for the capture and acceleration of plasma ions.

PACS numbers: 52.40.Mj, 52.35.Dm

1. INTRODUCTION

As is known, beams of charged particles are effective means for the excitation of waves in a plasma. The excitation of large-amplitude waves is accompanied by various nonlinear phenomena. One of the most widely investigated types of nonlinearity is at present the interaction of inhomogeneous hf (usually electron Langmuir) oscillations with a plasma via the force $\nabla E_{hf}^2(x, t)$ representing the pressure gradient of an hf field. This force produces slow (compared with the characteristic frequencies) changes in the plasma density and potential, facilitating the process of long-wavelength self-modulation of hf waves (if the Lighthill criterion¹ $\omega''(k)d\omega/da_0 < 0$, where a is the oscillation amplitude, is satisfied). Under certain conditions this results in collapse of growing localization of the hf oscillations accompanied by plasma expulsion. Another process being investigated, which is also due to the interaction between ∇E_{hf}^2 with a plasma, is the excitation of lf oscillations as a result of decay or nonlinear wave mixing. Nonlinear mixing of two hf waves of amplitudes $E_{1,2}$ and with frequencies and wave vectors $\omega_{1,2}$ and $k_{1,2}$ occurs when the following resonant interaction conditions are satisfied:

$$\Omega = \omega_1 - \omega_2, \quad \kappa = k_1 - k_2, \quad (1)$$

where Ω and κ are the frequency and wave vector of the lf oscillations. External excitation of hf oscillations makes it possible to generate readily the lf oscillations required for any specific purpose. The process of excitation of lf oscillations with the purpose of heating of a plasma in multibeam systems is considered in Ref. 2: as is known, beams can then generate hf oscillations of frequencies $\omega_n \approx \omega_{pe}$ when the condition $k_n \cdot v_{bn} = \omega_n$ is satisfied (n is the serial number of a beam, v_{bn} is the velocity of this beam, ω_{pe} is the electron plasma frequency, ω_n is the frequency of the wave excited by the beam and k_n is the wave vector of this wave). The wave frequency ω_n can be fixed by applying a weak modulating signal at the beam input and a resonant interaction with an lf wave, resulting in an effective transfer of energy to the plasma ions, can be achieved by varying the beam velocities.

There is also considerable interest in the problem of

collapse at high hf oscillation intensities, which has been discussed extensively by theoreticians (see, for example, Refs. 3–5) and has been studied experimentally on several occasions.^{6,7} The use of electron beams for the pumping of Langmuir oscillations makes it possible to vary the intensity of these oscillations within a wide range and to ensure conditions when formation of collapsing cavities becomes possible. However, in a confined plasma a beam excites electron space-charge waves, whose dispersion law is such that the Lighthill criterion is not obeyed by waves whose wave vectors are much smaller than the reciprocal of the Debye radius. Therefore, long-wavelength self-modulation and the associated collapse of cavities should not take place.

The excitation of lf oscillations by mixing of hf space-charge waves was investigated experimentally by Quon *et al.*⁸ and by Michelsen *et al.*⁹ They found qualitatively that the process agreed with the theoretical representations. Nevertheless, the details of the interaction mechanism between hf and lf waves, its effectiveness, possibility of its use for the heating of ions have not yet been investigated.

We shall report the results of an experimental investigation of plasma expulsion by hf space-charge waves, excited in a confined plasma column by two electron beams meeting head on. We studied in detail the mechanism of excitation of lf ion-acoustic waves by mixing of space-charge waves. We found that the ion-acoustic waves had an amplitude comparable with that of hf pump waves. This amplitude was sufficient for the capture and sufficient efficient heating of the ion component of the plasma.

The apparatus and the results are described in Sec. 2. They are discussed and compared with the theoretical ideas in Sec. 3, where conclusions are drawn.

2. EXPERIMENTS

The experiments were carried out using apparatus shown schematically in Fig. 1. Opposed hollow electron beams, of diameters 1 and 0.3 cm, passed through a tube 9 cm in diameter subjected to a homogeneous

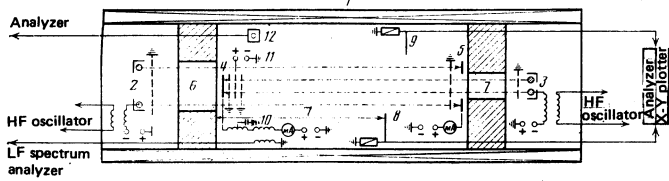


FIG. 1. Schematic diagram of the apparatus: 1) magnetic field solenoid; 2), 3) electron guns; 4), 5) collectors; 6), 7) channels creating pressure drops; 8) mobile probe; 9) immobile probe; 10) pulse transformer; 11) analyzing grid; 12) probe for analysis of ions.

magnetic field 500 Oe. These beams were created by guns 2 and 3. The electron emitters were tungsten filaments 0.05 cm thick. The beam energies were equal and amounted to 400 eV, which corresponded to a velocity of 1.18×10^9 cm/sec. The currents were received by collectors 4 and 5, which were subjected to a positive potential of the order of 20 V in order to suppress secondary emission; during these experiments these currents were 2.5–3.0 mA. The pressure in the working region was 1×10^{-4} Torr and near the cathodes it was an order of magnitude lower. This pressure drop was produced by channels 6 and 7 and by injecting a gas (helium, argon, or xenon) into the working part of the chamber. A plasma was created by ionization of the gas by the electron beams. The presence of different gases made it possible to create plasmas with different electron temperatures and ion masses. In the presence of helium and argon the electron temperature was $T_e = 13$ eV, whereas in the presence of xenon it was half this value ($T_e = 6.5$ eV).¹⁰

On increase in the pressure in the working chamber it was found that oscillations appeared in a narrow frequency band (of width $\sim 2\%$ of the main frequency) and this happened beginning from a certain threshold pressure. The amplitude of these oscillations and their frequency were independent of the nature of the gas but were governed by the electron currents injected into the system. A further increase in the pressure gave rise to a second oscillation region, separated by a frequency interval from the first, and the maximum of the oscillation intensity shifted to the second region. Further increase in the pressure produced a third oscillation region at higher frequencies and suppressed the first one; in this way it was possible to displace the oscillation region toward higher frequencies. These oscillation regions and the distribution of the hf potential along the length of the system in each region were recorded using mobile 8 and immobile 9 antenna probes made of tungsten wire 0.02 cm thick and connected to a load resistance equal to half the wave impedance of the cable. The signals produced by the probes passed through a selective amplifier and reached an X–Y plotter or directly a spectrum analyzer. Figure 2(a) (curve 1) illustrates the distribution of the hf potential along the system in the case when only the first oscillation region was observed.

The observed distribution indicated the appearance of a standing wave of the potential with a spatial period of 10 cm and with nodes at points 0, 10, 20, 30, and 40 cm. The smooth variation of the potential at the stand-

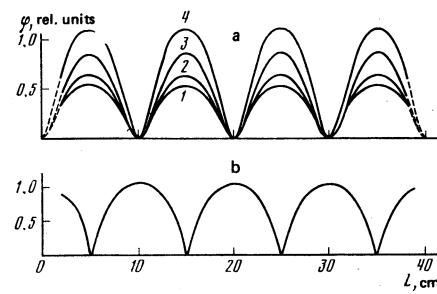


FIG. 2. Distributions of hf and lf potential along the system: a) distribution of the hf potential in the presence of initial modulation (1) and in the presence of a signal from an external oscillator (2, 3, 4); b) distribution of the lf potential.

ing-wave nodes was a spurious effect due to the detector. We thus found that at every moment there was an almost sinusoidal distribution of the potential in space. Neighboring antinodes corresponded to different signs of the potential [curve 1 in Fig. 2(a)]. Measurements carried out in the second and higher oscillation regions showed that the spatial period of the standing waves observed there decreased proportionally to the frequency ratio and amounted to 8.2 and 7 cm for the second and third regions. Thus, a wave of phase velocity $v_{ph} = 8.3 \times 10^8$ cm/sec and of wavelengths 20, 16.4, and 14 cm, respectively, was created in these regions. Clearly, the oscillation regions were separated by a frequency which was governed by the length of the plasma column and by the phase velocity of the excited waves. This frequency was 10 MHz and it was lowest for the system in question since half a wavelength could be fitted into the 40 cm working length of the system when v_{ph} had the value given above. We concluded that the opposed beams produced a standing wave pattern in the plasma column which then acted as a characteristic resonator. In the absence of the second beam the resultant perturbation drifted along the plasma column at the group velocity and the instability was of the drift (convective) nature. The second beam provided feedback in this system and resulted in an absolute instability causing the perturbation to grow with time at each point.

Since in the second stage of our investigation we studied only the first oscillation region, we should analyze in greater detail the oscillations in this region. The maximum amplitude of these oscillations was observed at 41.5 MHz and in this case the longitudinal wave vector was $k_{||} = 0.314$ cm⁻¹. We determined k_{\perp} bearing in mind that under experimental conditions we had $\omega_{Be}/2\pi \gg \omega_{pe}/2\pi$ (amounting to 1250 and 57 MHz, respectively), where ω_{Be} is the electron cyclotron frequency and the ratio of the beam densities to the plasma density is less than unity ($n_b/n_p = 2 \times 10^{-2}$). In this case the frequency of the excited oscillations was $\omega = \omega_{pe} \cos \theta$, where θ is the angle of inclination of the wave vector. Hence, we found that the transverse wave vector was $k_{\perp} = 0.3$ cm⁻¹.

As pointed out earlier, the oscillation amplitude in a given region was independent of the nature of the gas and, consequently, of the electron temperature, i.e., the amplitude had not yet reached the values at which

the plasma electrons were captured by the wave.¹⁰ Therefore, it was possible to increase the oscillation amplitude by initial modulation of the electron beams at a frequency whose intensity maximum was in the oscillation region. With this in mind we applied a signal from an external hf oscillator to the gun cathodes (via transformers). At any one given frequency it was sufficient to modulate one (either of the two) beams. In this case the spectrum of the observed oscillations narrowed down to the width of the signal of the external hf oscillator.¹¹ If two close frequencies were excited in the system, then each beam was modulated by its own frequency. Variation of the amplitude of the signal from the external oscillator provided means for controlling the oscillations established in the system. Curves 2, 3, and 4 in Fig. 2(a) illustrate an increase in the oscillation amplitude in a plasma column as a result of variation of the signal from an external hf oscillator.

We investigated the effect of the Langmuir oscillations of various amplitudes on the plasma density in the zones with the maximum electric field intensity. As indicated by Fig. 2(a), these zones were in the vicinity of the points with $L=10, 20,$ and 30 cm. The dependence of the electric field on the distance could be found by differentiating, with respect to the coordinate L , the distribution of the potential along the system [Fig. 2(a)]. One should bear in mind that the signs of the neighboring antinodes of the potential were opposite and one should exclude from the differentiation process the distribution of the potential near the nodal points distorted by the detector.

The plasma density was measured in the vicinity of the point $L=30$ cm as follows. Mobile and immobile probes (8 and 9 in Fig. 1) were located at the point $L=30$ cm on diametrically opposite sides of the column. Use was made of a resonance of this column subjected to a strong magnetic field.¹² A measuring signal from a variable-frequency oscillator was applied to one of the probes. The second probe was used as a signal detector. The dependence of the coupling between the probes (amplitude of the transmitted signal) on the frequency of the external oscillator was determined. When the frequency of this oscillator coincided with the resonance frequency ω_{res} (in the case considered $\omega_{res} = \omega_{pe}$), the coupling between the probes increased. We thus determined the plasma frequency and, therefore, the plasma density. Figure 3 shows the dependences of the coupling between the probes for different amplitudes of the oscillations established in the system. In this case the working gas was argon and the electron temperature was 13 eV. Without an external signal or for a low level of this signal [curves 1 and 2 in Fig. 2(a)] the resonance frequency, and consequently also the plasma frequency, were independent of the signal level and amounted to 57 MHz (curve 1 in Fig. 3). An increase in the oscillation amplitude shifted the resonance curve toward lower frequencies, as illustrated by curve 2 in Fig. 3 representing oscillations described by curve 4 in Fig. 2(a). The calculated relative change in the density $\delta n/n$ in the regions with the maximum intensity of the hf field was 7% in the case of argon and reached

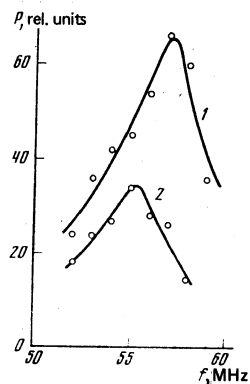


FIG. 3. Frequency dependences of the coupling between the probes (amplitude of the transmitted signal): 1) in the absence of initial modulation of the beam; 2) in the case of beam modulation for oscillation amplitudes corresponding to curve 4 in Fig. 2.

18% in similar experiments on xenon when the electron temperature was twice as low ($T_e = 6.5$ eV).

A study was made of the dynamics of plasma expulsion. The application of an external large-amplitude signal [curves 3 and 4 in Fig. 2(a)] resulted in simultaneous growth of the envelope of the hf signal and a reduction in the coupling between the measuring probes at the plasma resonance frequency. The interval between the beginning of a reduction in this signal and establishment of a new value represented the time during which a new density was established at a given point. Oscillograms of the hf signal envelope (a) and of the measuring signal used for various gases (b, c, d) are shown in Fig. 4. It is clear from these oscillograms that the time required for plasma expulsion varied with the gas: it was 4 μ sec for xenon, 10 μ sec for argon, and 20 μ sec for helium. The rise time of the hf oscillations was practically the same for all the gases and was governed by the rate of rise of the hf voltage applied to the cathode gun. The experimental

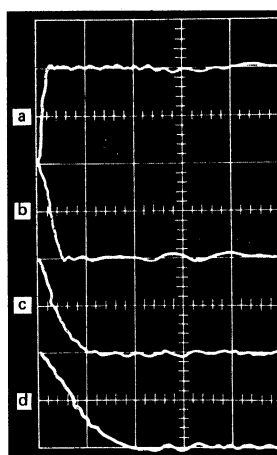


FIG. 4. Oscillograms of the envelopes of the main hf and measuring signals in different gases: a) envelope of the main hf signal in the case of xenon, argon, and helium; b), c), d) envelopes of the measuring signal in the case of xenon, argon, and helium, respectively. The horizontal scale is 10 μ sec/cm.

value of this time was $\sim 2 \mu\text{sec}$.

We also studied experimentally the interaction of two waves of different frequencies. In this case the cathodes of the guns 2 and 3 in Fig. 1 were subjected to signals from external oscillators and the frequencies of these signals differed by a few tens of kilohertz. Beats of frequency equal to the difference value were then observed in the plasma column. Typical oscillograms of such beats, observed for different oscillation amplitudes, are shown in Fig. 5. These oscillograms were obtained at the point $L=25 \text{ cm}$, where—as in the case of one external oscillator—there was a maximum of the hf potential. A study of the spatial distribution of this potential showed that in the presence of beats this distribution was identical with that shown in Fig. 2(a).

The same hf probes 8 and 9 (Fig. 1) were also used to study the time dependence of the plasma density at the point $L=30 \text{ cm}$. It was not convenient to use then the plasma column resonance because of the considerable width of the resonance curves (Fig. 3). Therefore, a more sensitive method was used. One of the probes was subjected to an hf signal of frequency $\omega/2\pi=1250 \text{ MHz}$, which was slightly higher than the electron cyclotron frequency ω_{Be} . The second probe acted as a receiver antenna. Since the refractive index of the plasma for waves with the right-hand polarization, traveling along a magnetic field, has a resonance at $\omega=\omega_{Be}$, the coupling between the probes near this frequency should exhibit a similar resonance. This is demonstrated in Fig. 6, showing the amplitude of the signal reaching the receiving probe as a function of the magnetic field. The curve is similar to that obtained for the refractive index near ω_{Be} in Ref. 13. The change in the plasma density resulted in a change in the refractive index; the higher the plasma density, the stronger was the coupling between the probes and the stronger the signal transmitted to the second probe; conversely, this caused amplitude modulation of the measuring signal. After detection the signal was applied to an oscilloscope. The behavior of the plasma density at the point $L=30 \text{ cm}$ had the form shown in Fig. 7 (curve b): the unperturbed value of the density corresponded to a maximum deflection of the oscilloscope beam from the zero value and the zero value cor-

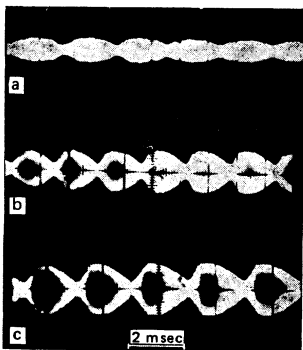


FIG. 5. Typical oscillograms of beats: a) oscillation amplitude corresponding to curve 2 in Fig. 2; b) oscillation amplitude corresponding to curve 3 in Fig. 2; c) oscillation amplitude corresponding to curve 4 in Fig. 2.

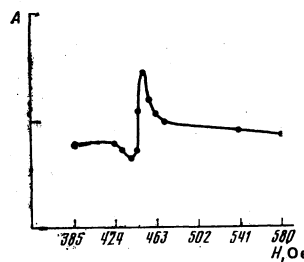


FIG. 6. Coupling between the probes (transmitted signal) at the frequency of 1250 MHz plotted as a function of the magnetic field.

responded to a reduced density. The envelope of the hf oscillations at the same point had the form represented by curve a in Fig. 7. Clearly, the two curves were in antiphase and the hf oscillation maxima corresponded to the density minima at the same moment. We thus concluded that the interaction of two hf waves resulted in modulation of the electron density at the beat frequency.

Oscillations of the potential in phase with oscillations of the electron density had the same frequency. These hf oscillations of the potential were sawtooth-shaped and had the negative polarity. Their spatial distribution was of the kind shown in Fig. 2(b). The phase of the hf signal was the same in all the regions of high hf field and when the hf oscillation amplitude increased, the amplitude of the hf signal increased quadratically. Variation of the frequencies of external hf oscillators in a fairly wide range of frequencies. There was a considerable interest in the cases when the difference frequency coincided with natural hf oscillations of the system. These hf oscillations were detected by the probe 8 (Fig. 1) and were then applied to a spectrum analyzer. A preliminary study identified natural hf oscillations in the absence of external signals. An investigation was made of the dependence of the hf oscillation spectrum on the nature of the gas and, consequently, on the electron temperature. This gave the spectra shown in Fig. 8 for argon (a), xenon (b), and helium (c). The spectra for argon and xenon were similar but they differed considerably from the case when helium ions were present in the system. The maximum noise amplitude in the case of argon and xenon was located higher than the ion cyclotron frequency, whereas in the case of helium the whole hf noise region was considerably lower. As reported in Ref. 14, in the presence of a magnetic field these hf oscillations had two branches (Fig. 9): the short-wavelength asymptote of the branch

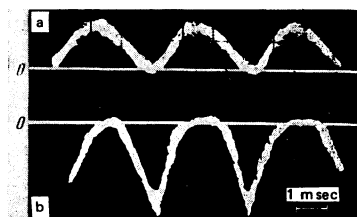


FIG. 7. Oscillograms of the envelopes of the hf oscillations and measuring signal: a) envelope of the hf oscillations corresponding to curve 4 in Fig. 2; b) envelope of the measuring signal.

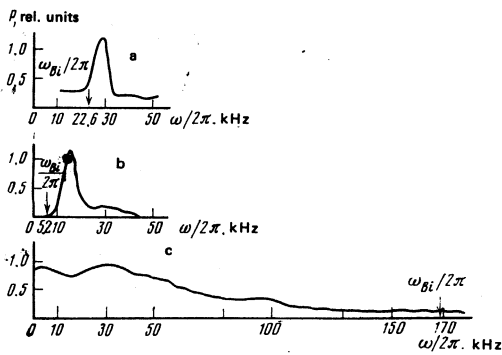


FIG. 8. Spectra of hf plasma oscillations in different gases: a) argon; b) xenon; c) helium.

a in Fig. 9 corresponded to the hf ionic sound and the long-wavelength asymptote of the branches *b* corresponded to ion-acoustic oscillations. We called these intervals of the hf oscillations the hf and lf ionic sound, respectively. The fact that only these oscillations appeared in the system was confirmed by a simple comparative analysis of the observed and calculated frequencies. Under our experimental conditions the velocity of sound in xenon was 2.06×10^5 cm/sec, and the corresponding velocities in argon and helium were 6.1×10^5 and 1.68×10^6 cm/sec. The amplitude of the observed oscillations was constant along the system, which was possible only if the condition $k_{\parallel} \ll k_{\perp}$ was obeyed; in estimates we could use the value $k_{\perp} = 0.3$ cm $^{-1}$ found experimentally from an analysis of the electron hf oscillations. The parameter $k_{\perp} v_s / \omega_{Bi}$ was 1.8 for xenon, 1.25 for argon, and 0.47 for helium (ω_{Bi} is the ion cyclotron frequency and v_s is the velocity of the ionic sound). The calculated oscillation frequencies $\omega/2\pi = kv_s/2\pi$ and the corresponding experimental values for xenon, argon, and helium, respectively were

Calculation:	10 kHz	29 kHz	80 kHz
Experiment:	14 kHz	29 kHz	much lower

A comparison of these results with the oscillation branches in Fig. 9 readily showed that the hf ionic sound was generated in xenon and argon (curve *a*) whereas strong ion-cyclotron damping was observed for the same branch in helium. The frequencies in helium, which were considerably lower than the ion-cyclotron frequencies, were due to the second branch of the dispersion curve in Fig. 9 representing the lf ionic sound (curve *b*). It should also be noted that the ratio of the effective Langmuir radius of ions, defined as $\rho = (T_e / m_i \omega_{Bi}^2)^{1/2}$, to the characteristic size of the

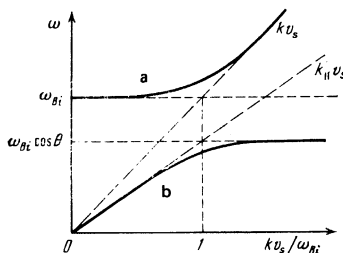


FIG. 9. Dispersion curves of ion-acoustic plasma oscillations a) hf oscillations; b) lf oscillations.

plasma inhomogeneity (equal in our case to the radius of the metal tube) was 1.33 for xenon, 0.91 for argon, and 0.35 for helium. As is known,¹⁵ when the condition $\rho/r > 1$ is satisfied, the instabilities with $\omega > \omega_{Bi}$ predominate, whereas in the $\rho/r < 1$ case we need consider only the lf long-wavelength perturbations ($\omega \ll \omega_{Bi}$).

In the case when the beat frequency of electron hf oscillations coincided with natural ion-acoustic oscillations, xenon and argon ions were accelerated along the magnetic field. The acceleration was observed up to frequencies $\sim \omega_{Bi}/2\pi \cdot \sqrt{2}$ (170 kHz for argon and 90 kHz for xenon), where ω_{Bi} is the ion plasma frequency. In the presence of lf ion-acoustic oscillations (in helium) there were no accelerated ions. An analysis of the accelerated ions was made in the collector circuit (4 in Fig. 1). The collector received electrons from the first beam as well as the plasma electrons. Application of a positive potential of the order of 20 V to the collector and a selection of the gap between the collector and the nearest grounded grid resulted in space-charge limitation of the plasma electron current in the gap. When a pulse of positive particles reached the gap, the space charge was partly compensated and this increased the electron current in the collector circuit. The resultant current peak was passed from the collector circuit to a pulse transformer (10 in Fig. 1). The pulse repetition frequency was equal to the frequency of the ion-acoustic oscillations and the pulses were applied to an lf spectrum analyzer. The energy composition of the ions was studied by the application of a positive potential to the grid (11 in Fig. 1). Unusual current-voltage characteristics were recorded and their coordinates were the readings of the spectrum analyzer for a positive potential on the grid 11. These characteristics are shown in Fig. 10(a) for argon ions at various difference frequencies. The acceleration to 20 eV was exhibited also by xenon ions but not by helium ions.

An analysis of the accelerated ions was made by another probe (12 in Fig. 1), located at the wall of the vacuum chamber. This probe was a trough with an aperture 0.4 cm in diameter covered by a metal grid of 97% transparency. Inside there was a receiving electrode, which was subjected to a positive potential

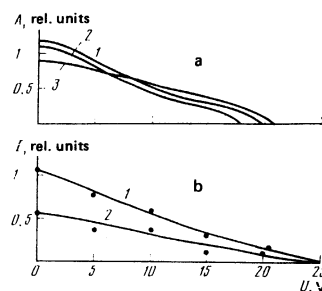


FIG. 10. Current-voltage characteristics obtained for various difference frequencies in the presence of argon in the system: a) characteristics recorded by the analyzer 11 in Fig. 1 at 44, 22.5 and 92 kHz (curves 1, 2, and 3, respectively); b) characteristics recorded by the analyzer 12 in Fig. 1 at 44 and 22.5 kHz (curves 1 and 2, respectively).

and which recorded the ion current. This probe was located so that the analyzing electric field was perpendicular to the magnetic field and the magnetic field was such that the ions in Larmor motion reached the probe aperture. The probe was located at a distance of 3.5 cm from the axis of the system at the point $L = 10$ cm. The receiving electrode circuit recorded ion current pulses at the beat frequency. The current-voltage characteristics recorded for argon at various beat frequencies had the form shown in Fig. 10(b). According to the calculations, the probe could receive particles with a transverse energy not exceeding 20 eV for argon. The observed energies up to 5 eV could be explained by the fact that the probe also received particles traveling at a small angle relative to its plane and, because of the edge effect of the analyzing field, the receiving electrode also recorded particles of energy close to the total ion energy.

3. DISCUSSION OF RESULTS AND CONCLUSIONS

The field of beam-excited space-charge waves can be represented as a superposition of the waves:

$$\begin{aligned} E(\mathbf{k}, t) &= E_{\mathbf{k}} \exp(i\mathbf{k}\mathbf{x} - i\omega_{\mathbf{k}}t) \\ + E_{\mathbf{k}-\boldsymbol{\kappa}} \exp(i(\mathbf{k}-\boldsymbol{\kappa})\mathbf{x} - i\omega_{\mathbf{k}-\boldsymbol{\kappa}}t) &= c.c. \end{aligned} \quad (2)$$

The frequency difference $\omega_{\mathbf{k}} - \omega_{\mathbf{k}-\boldsymbol{\kappa}}$ can be varied experimentally within a wide range. Our investigations showed that the hf field have a considerable influence on the distribution of the plasma electron density. The equation for a perturbation of the plasma density is¹⁶

$$\frac{\partial^2 n}{\partial t^2} - v_s^2 \Delta n = \frac{1}{8\pi m_i} \Delta E^2. \quad (3)$$

In the case when $\omega_{\mathbf{k}} = \omega_{\mathbf{k}-\boldsymbol{\kappa}}$ and $\mathbf{k} - \boldsymbol{\kappa} = -\mathbf{k}$, as well as $E_{\mathbf{k}} = E_{-\mathbf{k}}$, Eq. (2) yields the following equation for perturbation of the electron density with a spatial scale $\boldsymbol{\kappa} = 2\mathbf{k}$:

$$\left(\frac{\partial^2}{\partial t^2} + 4v_s^2 k^2 \right) \delta n_{2\mathbf{k}} = \frac{2k^2}{\pi m_i} E_{\mathbf{k}}^2. \quad (4)$$

Hence, a constant perturbation of the density is

$$\delta n_{2\mathbf{k}} = E_{\mathbf{k}} E_{-\mathbf{k}} / 2\pi v_s^2 m_i. \quad (5)$$

When the wave frequencies $\omega_{\mathbf{k}}$ and $\omega_{\mathbf{k}-\boldsymbol{\kappa}}$ do not coincide, Eq. (3) satisfies the solution for a density perturbation of the following kind:

$$\delta n(\boldsymbol{\kappa}, t) = \delta n(\boldsymbol{\kappa}) \exp(-i\Delta\omega t + i\boldsymbol{\kappa}\mathbf{x}), \quad (6)$$

where

$$\delta n(\boldsymbol{\kappa}) = \boldsymbol{\kappa}^2 E_{\mathbf{k}} E_{\mathbf{k}-\boldsymbol{\kappa}} / 2\pi m_i (\Omega_{\boldsymbol{\kappa}}^2 - \Delta\omega^2 + 2i\gamma_{\boldsymbol{\kappa}}\Omega_{\boldsymbol{\kappa}})$$

$\Omega_{\boldsymbol{\kappa}} = V_s \boldsymbol{\kappa}$, $\nabla\omega = \omega_{\mathbf{k}} - \omega_{\mathbf{k}-\boldsymbol{\kappa}}$, and $\gamma_{\boldsymbol{\kappa}}$ is the damping coefficient of the lf oscillations. It follows from Eq. (6) that in the case of interaction of two hf waves of different frequencies with a plasma the electron density is modulated at the different frequency $\Delta\omega$ and if this frequency coincides with the natural frequency of the system $\Omega_{\boldsymbol{\kappa}}$, a resonant increase in the modulation density takes place as a result of resonant mode merging [see Eq. (1)].

Modulation of the electron density gives rise to lf oscillations of the potential, whose amplitude is related to the change in the density in the case of the Boltzmann distribution:

$$\varphi_{lf} = \delta n T_e / ne. \quad (7)$$

The above relationship is valid at not too low values of k_{\parallel} when the phase velocities of the waves are considerably less than the thermal velocity of electrons. In the experiments when $\Delta\omega = 0$ this condition is known to be satisfied because the phase velocity vanishes and in the case of resonant excitation of lf oscillations ($\Delta\omega = \omega_{\mathbf{k}} - \omega_{\mathbf{k}-\boldsymbol{\kappa}}$) the ratio of the phase velocities of the excited lf oscillations to v_{Te} is of the order of 10^{-2} .

In the case when $\Delta\omega = 0$ the experimental data for the plasma expulsion together with Eqs. (4) and (5) can be used, if the hf and gas-kinetic pressure forces are equal, to estimate the hf oscillation amplitude from

$$|E|^2 = -16\pi T_e \delta n_{2\mathbf{k}}. \quad (8)$$

In the case of helium and argon, when $T_e = 13$ eV and $\delta n_{2\mathbf{k}}/n = 7\%$, the electric field intensity E_{hf} is 13.4 V/cm and the potential is then $\varphi_{hf} = 42.6$ V.

When $\Delta\omega$ differs from zero and accelerated xenon and argon ions are observed, the resultant lf potential can be estimated by analyzing the ion acceleration process. In the case of argon, ions are accelerated to energies of 20 eV and their velocity is 1.12×10^6 cm/sec. The inclined lf oscillations responsible for the acceleration are characterized by $k_{\perp} = 0.3$ cm⁻¹ and by a longitudinal wave vector $\boldsymbol{\kappa} = 2k_{\parallel} = 0.628$ cm⁻¹. The range of phase velocities corresponding to the acceleration process is $2 \times 10^5 - 10^6$ cm/sec. The acceleration of cold ions ($T_{i0} = 0$) occurs as a result of their capture by the lf wave field and subsequent motion together with the lf wave. The maximum attainable ion velocity is given by

$$v_{max} = v_{ph}^+ (2e\varphi_{lf} / m_i)^{1/2}. \quad (9)$$

When the condition for the capture of ions by the lf wave field is obeyed, we have

$$m_i (v_{ph}^- - v_{i0})^2 / 2 = e\varphi_{lf}. \quad (10)$$

When the phase velocity is 2×10^5 cm/sec, the capture of ions with $v_{i0} = 0$ requires, in accordance with Eq. (10), an lf potential $\varphi_{lf} = 0.6$ V. It follows from the observed ion velocities and from Eq. (9) that the lf wave amplitudes are at least 10.4 V. When the phase velocity was $v_{ph} = 10^6$ cm/sec, the capture amplitude is approximately 15 V and the maximum attainable velocity calculated from Eq. (9) is $\sim 2 \times 10^6$ cm/sec. The observed ion energies showed that the maximum energy acquisition was not achieved since the time taken by a wave to move across the system was less than one oscillation period of a captured particle.

It follows that when the difference frequency $\Delta\omega$ lies in the region of hf ionic sound of the system, the observed amplitudes of the lf potential indicate a resonant increase in the density modulation in accordance with Eq. (6) since the value of $\delta n/n$ calculated from Eq. (7) is 90%.

As pointed out earlier, lf long-wavelength oscillations are excited in helium and in this case the condition for resonant merging of modes (1) is not obeyed and the resonant increase in the density modulation does not occur. The lf amplitudes of 0.8 V, resulting from 7% nonresonance density modulation, are suffi-

cient simply for the acceleration of helium ions to energies of the order of 2 eV, which is below the sensitivity threshold of the techniques employed by us.

In spite of the fact that plasma expulsion by the hf field and formation of low-density regions are observed experimentally, localization of the electric fields does not take place. This is clear from Fig. 2(a) (the form of the distribution of the hf potential in space is independent of the oscillation level) and also from an analysis of the oscillograms of the time beats [Figs. 5(b) and 5(c)]. In spite of the fact that the shape of the envelope differs considerably from sinusoidal, no peaking of the envelope is observed.

In considering the effective excitation of lf oscillations we have to allow for the dynamics of expulsion of the electron density by the hf field. The observed difference between the dynamics of expulsion of helium and xenon plasmas can be explained if we bear in mind that the ratios of the Larmor radii of helium and xenon ions to the radius of the plasma column ρ_i/r are very different. For helium we have $\rho_i/r=0.35$, whereas for xenon we have 1.35 and for argon we have 0.91. This means that in the case of expulsion of a helium plasma the rate of the process is governed by the velocity of ions along the plasma column, which does not exceed the ionic sound velocity (helium ions can be regarded as magnetized). The process of expulsion of argon (and particularly xenon) plasma is faster because its rate is governed by the velocity of transverse drift of ions out of the plasma column. In this case such ions are not magnetized and we have $v_{Li} \approx v_{Ti}$. It is clear from Fig. 4 that the velocity of transverse drift of ions is considerably greater than the velocity of ambipolar diffusion along a magnetic field.

Our investigation has made it possible to establish details of the process of plasma expulsion by the ponderomotive force of hf space-charge waves. It has been found that multibeam systems provide effective means for resonant excitation of lf oscillations in a wide range of frequencies and wave vectors. It is shown that in the case of resonant merging of plasma oscillation modes it is possible to excite lf waves whose amplitudes are comparable with the amplitudes of mixed space-charge waves. A strong interaction of

lf waves with ions and heating of the latter to significant energies show that such systems can be used for efficient plasma heating.

The authors are grateful to M. V. Nezlin for valuable discussions and comments.

- ¹M. J. Lighthill, *J. Inst. Math. Appl.* **1**, 269 (1965).
- ²A. S. Bakai, *Voprosy teorii nelineinykh kolebaniĭ i ikh primeneniĭ v fizike (Problems in the Theory of Nonlinear Oscillations and Their Applications in Physics)*, Preprint KhFTI 71-4, Kharkov, 1971.
- ³V. E. Zakharov, *Zh. Eksp. Teor. Fiz.* **62**, 1745 (1972) [*Sov. Phys. JETP* **35**, 908 (1972)].
- ⁴A. A. Galeev, R. Z. Sagdeev, Yu. S. Sigov, V. D. Shapiro, and V. I. Shevchenko, *Fiz. Plazmy* **1**, 10 (1975) [*Sov. J. Plasma Phys.* **1**, 5 (1975)].
- ⁵V. V. Gorev and A. S. Kingsep, *Fiz. Plazmy* **1**, 601 (1975) [*Sov. J. Plasma Phys.* **1**, 332 (1975)].
- ⁶A. Y. Wong and B. H. Quon, *Phys. Rev. Lett.* **34**, 1499 (1975).
- ⁷S. V. Antipov, M. V. Nezlin, E. N. Snezhkin, and A. S. Trubnikov, *Zh. Eksp. Teor. Fiz.* **76**, 1571 (1979) [*Sov. Phys. JETP* **49**, 797 (1979)].
- ⁸B. H. Quon, A. Y. Wong, and B. H. Ripin, *Phys. Rev. Lett.* **32**, 406 (1974).
- ⁹P. Michelsen, H. L. Pecseli, J. J. Rasmussen, and N. Sato, *Phys. Fluids* **20**, 1094 (1977).
- ¹⁰V. D. Fedorchenko, Yu. P. Mazalov, and B. N. Rutkevich, *Zh. Tekh. Fiz.* **43**, 710 (1973) [*Sov. Phys. Tech. Phys.* **18**, 448 (1973)].
- ¹¹Ya. B. Fainberg, *At. Energ.* **13**, 313 (1961).
- ¹²R. Huddlestone and S. L. Leonard (eds.), *Plasma Diagnostic Techniques*, Academic Press, New York, 1965 (Russ. Transl., Mir. M., 1967, p. 400).
- ¹³R. Huddlestone and S. L. Leonard (eds.), *Plasma Diagnostic Techniques*, Academic Press, New York, 1965 (Russ. Transl., Mir. M., 1967, p. 400).
- ¹⁴A. B. Mikhailovskii, *Teoriya plazmennykh neustoĭchivostei (Theory of Plasma Instabilities)*, Vol. 1, Atomizdat, M., 1950, p. 150.
- ¹⁵A. B. Mikhailovskii, *Teoriya plazmennykh neustoĭchivostei (Theory of Plasma Instabilities)*, Vol. 2, Atomizdat, M., 1977, p. 202.
- ¹⁶A. A. Vedenov and L. I. Rudakov, *Dokl. Akad. Nauk SSSR* **159**, 767 (1964) [*Sov. Phys. Dokl.* **9**, 1073 (1965)].

Translated by A. Tybulewicz